ELSEVIER

Journal of Nuclear Materials 253 (1998) 60–66

journal of nuclear materials

Dimensional stability and tensile strength of irradiated Nicalon-CG and Hi-Nicalon fibers

C.H. Henager [a,*], G.E. Youngblood [a], D.J. Senor [a], G.A. Newsome [b], J.J. Woods [b]

[a] *Pacific Northwest National Laboratory [1], P.O. Box 999, Richland, WA 99352, USA*
[b] *Lockheed Martin, P.O. Box 1072, Schenectady, NY 12301, USA*

Abstract

Nicalon-CG and Hi-Nicalon fibers were characterized by measuring their density and tensile strength in the unirradiated, thermal annealed, and irradiated conditions. The results indicate the fibers that perform best after irradiation to 43 dpa SiC at 1000°C are those that approach stoichiometric and crystalline SiC. Hi-Nicalon fiber exhibited less than 1% densification, accompanied by a slight increase in tensile strength after irradiation. Nicalon-CG, in contrast, was significantly weakened in the annealed and irradiated conditions. In addition, Nicalon-CG exhibited substantial irradiation-induced shrinkage. Loss of fiber tensile strength after irradiation is shown to reduce the flexural strength of irradiated composites while fiber shrinkage, and resultant debonding from the matrix, are linked to a reduced composite elastic modulus. © 1998 Elsevier Science B.V.

1. Introduction

Silicon carbide (SiC) materials in the form of SiC-fiber-reinforced/SiC matrix (SiC_f/SiC) composites combine non-catastrophic failure modes analogous to the plastic deformation of traditional metallic materials [1,2] with minimal nuclear activation and afterheat [3–7]. As a result, SiC_f/SiC composites are under consideration as structural materials in several fusion reactor concepts [3–6]. However, many issues must be addressed before their inclusion in detailed designs, including lower cost fabrication methods and more complete characterization of the effect of irradiation on material properties [8]. The purpose of the present study is to examine the microstructural, dimensional, and strength properties of a selection of SiC-based fibers after neutron irradiation at elevated temperatures and high fluences [9,10].

2. Experimental

2.1. SiC-based fibers

Table 1 lists the fibers examined in the present study along with relevant property and microstructural data provided by the manufacturers. Nicalon-CG fibers contain a significant concentration of oxygen, which is introduced during pyrolysis; the Hi-Nicalon fibers are electron beam cured, thus reducing the introduction of oxygen. The presence of excess carbon and oxygen cause the Nicalon-CG fibers to be partially amorphous. The Hi-Nicalon fibers are more crystalline, but still contain excess carbon. The Nicalon-CG fiber was examined without a coating, and with 150 nm pyrolitic carbon (PyC), 15 nm PyC, and 150 nm BN coatings.

2.2. Irradiation and thermal anneal conditions

The irradiation was conducted in the EBR-II, in an inert gas atmosphere at approximately 1000°C, for 185 effective full power days (EFPD), resulting in a fluence of 3.4×10^{22} n/cm^2 ($E > 0.1$ MeV). The fluence value was determined

* Corresponding author. Tel.: +1-301 903 8230; fax: +1-301 903 9513; e-mail: chuck.henager@oer.doe.gov.

[1] Pacific Northwest National Laboratory is operated for the US Department of Energy by Battelle Memorial Institute under contract DE-AC06-76RLO 1830.

PII S0022-3115(97)00322-X

Table 1
Fiber properties

Fiber	Vendor	Composition (w/o)	Density (g/cm^3)	Strength (GPa)	Modulus (GPa)	Microstructure
Nicalon-CG	Nippon Carbon	Si–31C–12O	2.55	2.6	190	2 nm β-SiC grains and free C in amorphous Si–O–C matrix
Hi-Nicalon	Nippon Carbon	Si–36C–0.5O	2.74	2.8	270	5 nm β-SiC grains and free C

from neutron activation analysis of a dosimetry capsule and corresponds to a dose of 43 dpa SiC in the EBR-II neutron spectrum, assuming threshold displacement energies of 25 eV for Si and 31 eV for C. To separate possible thermal stability effects due to the 1000°C exposure during irradiation, a duplicate set of fibers was held at 1010°C for 165 days in an inert gas atmosphere in the absence of irradiation.

2.3. Fiber density

The fiber density for unirradiated, annealed, and irradiated conditions was measured on a representative segment ($\approx$ 1 cm long) cut from each of the fiber bundles using a liquid density gradient column technique [8]. Appropriate mixtures of carbon tetrachloride (CCl_4), bromoform ($CHBr_3$) and methylene iodide (CH_2I_2) were used to create the density gradient. The fiber bundles were inserted at the top of the column separately and allowed to sink to their equilibrium density; this typically required several hours. After reaching their equilibrium position, the fibers remained stationary in the column, and their average position and spread were recorded over a period of at least 24 h. The individual columns were mixed such that the highest and lowest density glass beads were no closer to the column ends than approximately 2 cm, and all fiber samples were suspended between these two extremes. Thus, the measured densities were always interpolated between two calibrated beads in the linear portion of the gradient column. Each column encompassed a 0.4 g/cm^3 density range over a 100 cm length; therefore, a number of columns with different liquid mixtures were necessary to cover the expected fiber density range of 2.0 to 3.1 g/cm^3. The density gradient in each column was quantified by correlating the densities of at least five calibrated glass beads with their axial positions in the column. Except for approximately 1 cm at each end, the density gradients in each column were linear. Based on typical observed spreading of the fiber fragments and the linearity of the density gradient, the precision of the density measurements is considered to be $\leq \pm 0.003$ g/cm^3 overall.

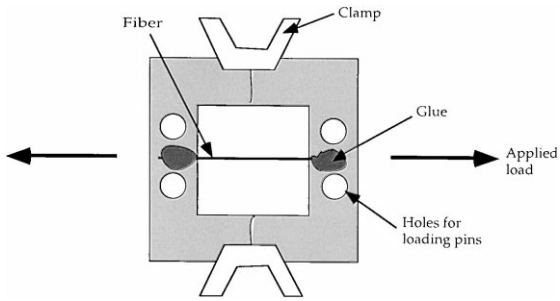

Fig. 1. Fiber tensile test fixture schematic.

2.4. Fiber tensile properties

Fiber tensile strengths were measured at room temperature using a computer controlled Micropull [2] load frame. Individual fibers with a nominal gage length of 2.54 cm were mounted and aligned on cardboard fixtures, as shown in Fig. 1. The cardboard fixture was cut on both sides, and the two pieces were held together with clamps. A single fiber was placed across the fixture and secured at both ends with a drop of thermosetting glue. To prevent the fibers from pulling away from the glue before reaching failure load, the glue covered at least a 0.60 cm length of the fiber end. The glue-mounted fibers were allowed to set for several hours before the fiber tensile tests. The holes in the cardboard fixture were then placed over loading pins in the test frame to ensure proper alignment. Then, the clamps were carefully removed so that the fiber carried the entire load. Load was applied at a constant strain rate of 2.0×10^{-4} s^{-1} until fiber failure. The fiber diameters were determined by scanning electron microscopy (SEM) examination of the fiber fragment protruding from one of the glued ends. The total number of tests for each fiber type and condition varied from 19 to 24 and was restricted by the quantity of irradiated fiber.

3. Results and discussion

3.1. Fiber dimensional stability

The bulk volumetric shrinkage of a fiber due to irradiation may be determined by measuring its pre- and post-irradiation densities. If the mass of the fiber is assumed to

[2] Micropull Science, Thousand Oaks, CA 91360, USA.

Table 2
Measured density changes and predicted dimensional changes using Eq. (3) for thermal annealed and irradiated fibers

Fiber type/interface	Thermal annealed		Irradiated		
	measured density change (%)	predicted length change (%)	measured density change (%)	predicted length change (%)	predicted diameter change (%)
Nicalon-CG (1)	0.84 ± 0.45	-0.28 ± 0.15	8.53 ± 0.39	-2.84 ± 0.13	-2.84 ± 0.13
Nicalon-CG (2)	1.14 ± 0.48	-0.38 ± 0.16	10.28 ± 1.28	-3.43 ± 0.43	-3.43 ± 0.43
Nicalon/15 nm PyC	0.04 ± 0.03	-0.01 ± 0.01	9.66 ± 0.49	-3.22 ± 0.16	-3.22 ± 0.16
Nicalon/150 nm PyC (1)	0.95 ± 0.13	-0.35 ± 0.04	10.13 ± 0.40	-3.38 ± 0.13	-3.38 ± 0.13
Nicalon/150 nm PyC (2)	1.64 ± 0.08	-0.55 ± 0.03	9.40 ± 0.53	-3.13 ± 0.18	-3.13 ± 0.18
Nicalon/150 nm BN	0.48 ± 0.13	-0.16 ± 0.04	12.36 ± 0.41	-4.12 ± 0.14	-4.12 ± 0.14
Hi-Nicalon	-0.25 ± 0.20	0.08 ± 0.07	0.67 ± 0.39	-0.22 ± 0.13	-0.22 ± 0.13

remain constant during irradiation, then the bulk volumetric shrinkage may be represented as

$$\frac{\Delta V}{V_0} \approx -\frac{\Delta \rho}{\rho_0}, \tag{1}$$

where V and ρ represent volume and density, respectively. The assumption of constant fiber mass is made to simplify the following derivation. However, there has been no attempt to verify this assumption to the best of our knowledge. If one further assumes that the fiber is cylindrical and contains no open porosity, Eq. (1) may be expanded and rearranged to yield

$$\frac{\Delta \rho}{\rho_0} + \frac{\Delta L}{L_0} + 2\frac{\Delta D}{D_0} \approx 0, \tag{2}$$

where L and D represent length and diameter, respectively. The diameter change due to irradiation is of significant interest for composite design because the fibers can debond from the matrix when shrinkage occurs. Unfortunately, this quantity can be difficult to measure reliably when there are large variations in as-fabricated fiber diameters and the presence of irregular cross sections. Nicalon-CG is more irregular in cross section than Hi-Nicalon, in general. If accurate density and length change measurements can be made, the expected diameter change can be calculated using Eq. (2). However, fiber length changes are difficult to perform accurately since fiber bending, twisting, etc., easily occur. Therefore, isotropic shrinkage is usually assumed and for fibers whose irradiation-induced shrinkage is isotropic, the expression in Eq. (2) can be reduced to

$$\frac{\Delta D}{D_0} = \frac{\Delta L}{L_0} = -\frac{1}{3}\frac{\Delta \rho}{\rho_0} \tag{3}$$

which allows the use of density measurements alone to determine the diametral changes and to estimate the length changes.

The measured fiber density changes due to the thermal annealing and irradiation are used to estimate fiber length and diameter changes using Eq. (3) with the assumption of isotropic dimensional change (Table 2). Thermal annealing at 1010°C for a comparable period as the irradiation exposure generally resulted in a slight increase in density ($\approx 1\%$) for the uncoated or coated Nicalon-CG fibers. This results in an approximately 0.3% to 0.5% predicted linear shrinkage when using Eq. (3). In contrast, the irradiation-induced predicted axial shrinkage is 3% to 4%. The Hi-Nicalon fibers exhibited less than 1% density change either due to the thermal anneal or to the irradiation ($\approx 0.2\%$ predicted length change). Presumably, this was due to the more crystalline nature of this fiber type. A comparison of the irradiated fiber diametral changes calculated using

Table 3
Summary of fiber tensile strength data

Fiber	Condition	Weibull scale parameter (GPa)	Weibull modulus	Apparent elastic modulus (GPa)[a]	Weibull distribution correlation coefficient
Nicalon-CG	unirradiated	3.37	2.87	159	0.992
	annealed	3.01	2.87	164	0.946
	irradiated	2.23	3.69	180	0.972
Hi-Nicalon	unirradiated	2.67	3.38	208	0.945
	annealed	2.30	6.41	225	0.979
	irradiated	3.92	5.15	258	0.975

[a] Determined from elastic loading slope during fiber test.

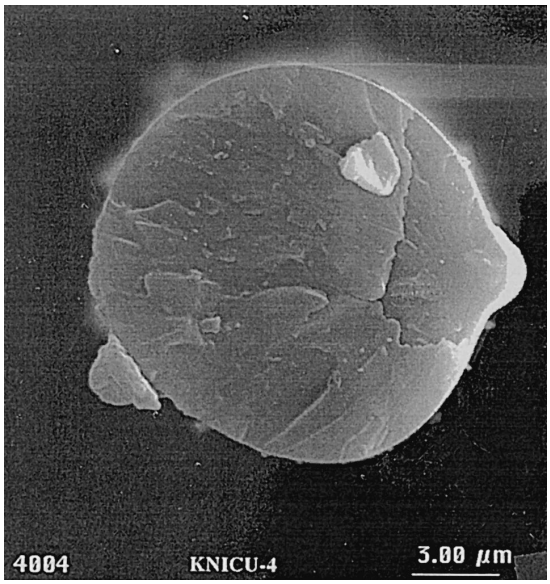

Fig. 2. Typical fiber tensile fracture surface appearance (unirradiated Nicalon-CG fiber).

measured density changes reveals that, under the assumptions of isotropic shrinkage, Hi-Nicalon is indeed superior to Nicalon-CG. The presence of a PyC or boron nitride (BN) coating does not greatly influence the measured density changes or, therefore, the estimated diameter changes.

3.2. Fiber tensile strength

The Weibull theory of statistical fracture applies well to ceramic fibers. To characterize the fracture behavior of brittle ceramic fibers, the following two parameter empirical distribution function is typically used [11–16]:

$$P_F = 1 - P_S = 1 - \exp\left(-(\sigma/\sigma_0)^m\right), \quad (4)$$

where P_F is the failure probability P_S is the survival probability for a fiber of length L under an applied stress (σ). The fit coefficients m and σ_0 are referred to as the Weibull modulus and scale parameters, respectively. The Weibull parameters are determined by performing a sufficiently large number of tests on a representative set of fibers of the same length, and fitting the results with Eq. (4) using a suitable estimator for P_F. From the fiber tensile tests, the failure strength (σ_f) of N fibers was obtained and a Weibull analysis was performed using the estimator

$$P_F = \frac{i}{N+1} \quad (5)$$

which is a recommended estimator [14]. The total number of fibers was restricted by availability of irradiated fibers and was fewer than the recommended number of about 30 for valid Weibull statistical information. Nonetheless, the data are indicative of trends for the effects of irradiation on fiber strengths.

A summary of the room temperature tensile strength data measured for uncoated Nicalon-CG and Hi-Nicalon fibers is given in Table 3. The fibers displayed nearly perfect elastic tensile behavior. The slope of the stress–displacement curves obtained using the fiber testing equipment and fixture described above is used as a guide to the relative fiber moduli and is referred to as the apparent elastic modulus in the table. It is less than the actual elastic modulus because it includes the compliance of the fixtures and test machine; however, it is useful as a relative guide. All fibers tested obeyed Weibull statistics, as expected, indicated by the relatively high correlation coefficients. No

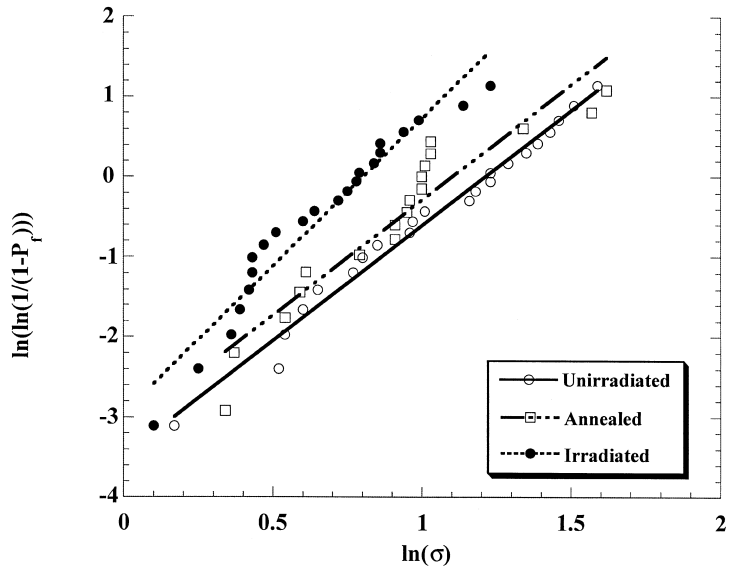

Fig. 3. Frequency of fiber failures as functions of applied stress and fiber condition for Nicalon-CG.

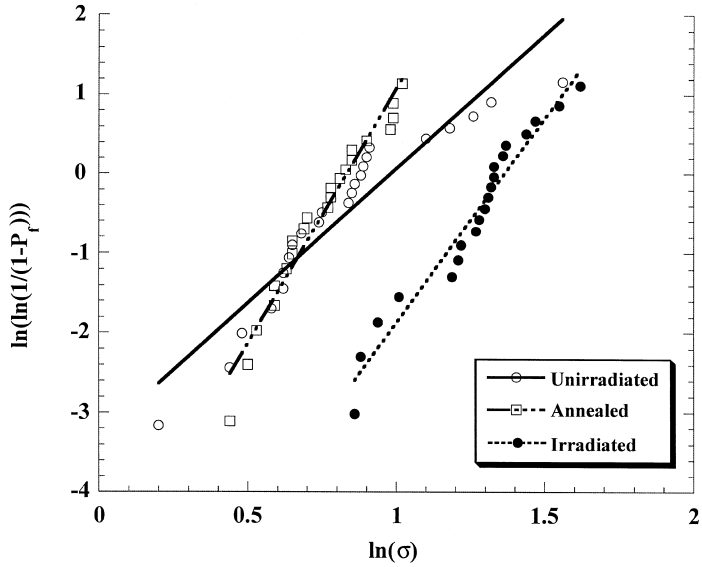

Fig. 4. Frequency of fiber failures as functions of applied stress and fiber condition for Hi-Nicalon.

differences were observed in subsequent SEM observations of fracture surfaces for any of the fibers in the unirradiated, annealed, or irradiated conditions. All examined fracture surfaces showed classic brittle cleavage fracture and the fibers usually broke into several segments at failure. A typical fracture surface is shown in Fig. 2. Generally, a segment remained protruding from the glue after fiber fracture. This segment was used to determine the individual fiber diameter by SEM examination for subsequent fiber stress calculation, but does not necessarily represent the initial fracture point.

The Weibull modulus for all fibers was relatively low (2.87–6.41), which is indicative of a wide variation in fracture strengths. The Weibull moduli are higher for Hi-Nicalon than for Nicalon-CG, which indicates better repeatability and more uniform fracture strengths. Nicalon-CG exhibits a decrease in strength from 3.37 to 3.01 GPa (as indicated by the Weibull scale parameter) due to the anneal, and a further decrease in strength to 2.23 GPa due to irradiation. The strength of unirradiated Hi-Nicalon is 2.67 GPa, lower than that for unirradiated Nicalon-CG, and Hi-Nicalon also exhibits a slight decrease in strength

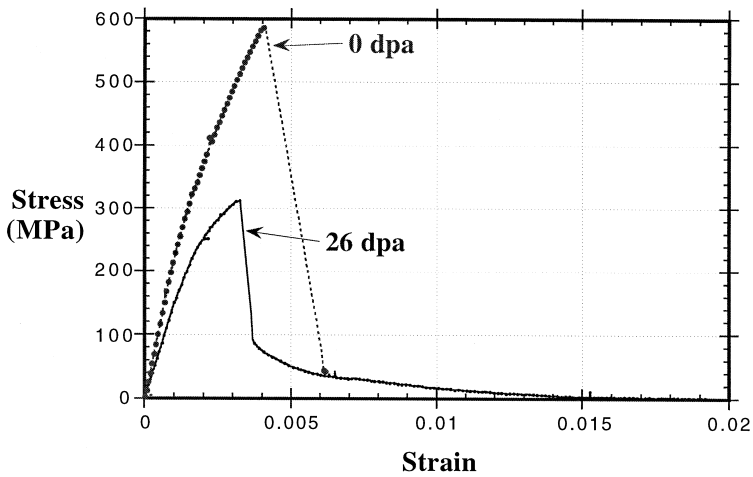

Fig. 5. Stress–strain curve in flexure for Nicalon-CG fiber composite tested at 800°C in Ar at 0 and 26 dpa SiC, respectively. Composite is 8-ply 0/90 plain weave with a CVI-SiC matrix.

to 2.30 GPa due to the anneal. After irradiation, Hi-Nicalon actually increases in strength to 3.92 GPa, which is higher than either unirradiated Hi-Nicalon or Nicalon-CG. The apparent elastic moduli for Nicalon-CG and Hi-Nicalon increase only slightly due to the anneal, but increase more due to irradiation. In general, the apparent elastic moduli for Hi-Nicalon are higher than Nicalon-CG, as expected for this more crystalline and elastically stiffer fiber.

The frequency of fiber failure as functions of applied stress and fiber condition for Nicalon-CG and Hi-Nicalon is shown in Figs. 3 and 4, respectively. In these figures, a shift to the left, as exhibited by Nicalon-CG after annealing and irradiation, indicates a general decrease in strength. In contrast, the data for Hi-Nicalon shift to the right after irradiation, which clearly illustrates the increase in strength indicated by the Weibull scale parameter.

Fig. 6. Scanning electron microscopy of machined surfaces of the Nicalon-CG composites tested above in Fig. 5. Composite in (a) is unirradiated and Nicalon-CG fiber is well-bonded and flush with the surface. Composite in (b) is irradiated to 26 dpa SiC and Nicalon-CG fiber is inset and debonded.

3.3. Effects on composite strength

Since the peak strength of woven SiC_f/SiC composites has been shown to depend directly on the fiber strengths, it is reasonable to expect that fiber strength reductions will affect measured composite strengths. This is indeed the case, as shown in Fig. 5, when a comparison between irradiated and unirradiated composite materials (otherwise identical) is made. The material is a Nicalon-CG-fiber, plain weave, 0/90 weave orientation, chemical vapor infiltration (CVI) SiC-matrix composite. Flexure strengths (4-point flexure) were measured at 800°C in pure Ar at a strain rate of 1.8×10^{-5} s^{-1} using 40 mm lower and 20 mm upper bending span dimensions. The measured strength reduction is about 47%, which compares to the 34% decrease (from 3.37 to 2.23 GPa in Table 3) in fiber tensile strengths measured in the single fiber tensile test. This correlation is some of the first direct evidence that fiber fracture strengths reduced by irradiation have a direct influence on composite fracture strengths [8].

3.4. Fiber density effects on composite integrity

The volumetric shrinkage of the Nicalon-CG fibers was first observed during microscopy of irradiated composites (as shown in Fig. 6). Fibers embedded in the CVI matrix were observed to have shrunk axially, and appeared inset into the composite surface as in Fig. 6(b), and radially, which causes the fibers to debond from the CVI matrix. The debonding was hypothesized to effect the composite stiffness, total elongation, and failure mechanism of the composite past the peak fracture stress [8]. It remains to be determined if the smaller shrinkage of the Hi-Nicalon fibers prevents debonding from the matrix as observed with the Nicalon-CG fibers.

4. Summary and conclusions

In general, the results of this study indicate that the fibers that perform best in an irradiation environment are those that approach stoichiometric and crystalline SiC, such as Hi-Nicalon compared to Nicalon-CG. Hi-Nicalon exhibited a small amount densification, accompanied by an increase in tensile strength after irradiation. However, the apparent dimensional stability of Hi-Nicalon fibers could be produced as an artifact of anisotropic shrinkage and swelling, as in graphite fibers. The differences between the irradiation performance of Nicalon-CG and Hi-Nicalon are most likely due to differences in compositional and microstructural characteristics. Other fibers with compositions even closer to stoichiometric SiC may also exhibit good, or perhaps even better, irradiation performance. The decreased fiber tensile strength of Nicalon-CG fibers was correlated to measured strength decreases in composites

fabricated from Nicalon-CG fibers. Strength and stiffness tests on irradiated composites fabricated with Hi-Nicalon fibers are required before the degree of fiber/matrix debonding and its subsequent effects on fiber properties can be determined.

Acknowledgements

The technical assistance of Drs J.L. Brimhall and J.R. Porter was very helpful.

References

[1] A.G. Evans, Mater. Sci. Eng. A 143 (1–2) (1991) 63.
[2] A.G. Evans, Philos. Trans. R. Soc. London, Ser. A 351 (1697) (1995) 511.
[3] G.W. Hollenberg, R.H. Jones, G.E. Lucas, Fusion Technol. 19 (3, Pt. 2B) (1991) 1701.
[4] L.L. Snead, Fusion Technol. 24 (1) (1993) 65.
[5] R.H. Jones, C.H. Henager Jr., J. Nucl. Mater. 212–215 (1994) 830.
[6] R.H. Jones, C.H. Henager Jr., J. Nucl. Mater. 219 (1995) 55.
[7] L.L. Snead, R.H. Jones, A. Kohyama, P. Fenici, J. Nucl. Mater. 233–237 (1996) 26.
[8] G.W. Hollenberg, C.H. Henager Jr., G.E. Youngblood, D.J. Trimble, S.A. Simonson, G.A. Newsome, E. Lewis, J. Nucl. Mater. 219 (1995) 70.
[9] D.J. Senor, G.E. Youngblood, J.L. Brimhall, G.A. Newsome, J.J. Woods, Fusion Technol. 30 (3) (1997) 956.
[10] G.E. Youngblood, D.J. Senor, G.W. Hollenberg, Fus. Mater. Semiannual Prog. Rep., DOE/ER-0313/18, US Department of Energy, 1995.
[11] K. Goda, H. Fukunaga, J. Mater. Sci. 21 (12) (1986) 4475.
[12] K. Okamura, T. Matsuzawa, M. Sato, Y. Higashiguchi, S. Morozumi, A. Kohyama, J. Nucl. Mater. 141–143 (1986) 102.
[13] K.K. Phani, Cent. Glass Ceram. Res. Inst. Bull. 34 (2) (1987) 33.
[14] S.N. Patankar, J. Mater. Sci. Lett. 10 (1991) 1176.
[15] H.F. Wu, A.N. Netravali, J. Mater. Sci. 27 (12) (1992) 3318.
[16] Y. Matsuo, J.X. Li, S. Kimura, Adv. Comp. Mater. 2 (1) (1992) 17.